Indian Journal of Chemistry
Vol. 63, January 2024, pp. 21-32
DOI: 10.56042/ijc.v63i1.785

Quantum chemical calculations, molecular docking and ADMET studies of *trans*-4-(trifluoromethyl)cinnamic acid

S Jeyavijayan*[a], M Ramuthai[b] & A Shiney[c]

[a] Department of Physics, Kalasalingam Academy of Research and Education, Krishnankoil 626 126, Tamil Nadu, India

[b] Department of Physics, Arumugham Palaniguru Arts and Science College for Women, Chatrapatti 626 102, Tamil Nadu, India

[c] Department of Physics, Pocker Sahib Memorial Orphanage College, Tirurangadi, Malappuram, Kerala 676 306, India

E-mail: sjeyavijayan@gmail.com

Received 24 April 2023; accepted(revised) 18 December 2023

trans-4-(Trifluoromethyl) cinnamic acid (4TFCA) has a -C=C- double bond among the aromatic system and the carboxyl ring which disturbed the π-electrons of the molecule. The geometrical parameters of 4TFCA is computed using the DFT/B3LYP by higher basis set (6-311++G(d,p)) and the frontier molecular orbital analysis is achieved. FTIR and FT-Raman spectra of 4TFCA have been obtained in the regions 4000-400 cm^{-1} and 4000-50 cm^{-1}. The experimental vibrational frequencies are in good coordination with the calculated wavenumbers. The absorption spectra of 4TFCA have been calculated by using the time dependent/density functional theory approach. The stability of a molecule rising from hyper-conjugative π →π* exchanges and charge delocalization has been calculated using natural bond orbital (NBO) analysis. The thermodynamic and charge responses have been studied. In addition, the results of molecular docking reveal that the molecule 4TFCA has the highest binding energy (–6.10 kcal/mol) with the histone deacetylase inhibitor (HDAC8). To understand the molecule's drug likeness, ADMET analysis has also been studied.

Keywords: DFT, *trans*-4-(Trifluoromethyl)cinnamic acid, Vibrational assignments, Docking, ADMET

Cinnamic acid (CA) is known as phenyl acrylic acid or benzal acetate, is a chemical compound, found in cinnamon, a common dietary spice[1]. Aqueous cinnamon extract (ACE), which induces apoptosis in the SiHa cell line *via* loss of mitochondrial membrane potential, has been previously reported to have chemo preventative potential in cervical cancer[2]. Many of pharmacological properties of cinnamon have been reported, including anti-inflammatory, antibacterial[3] and anticancer activities[4]. Recently, the electronic interactions of cinnamic acid derivatives have been carried out by DFT calculations[5]. Histone deacetylases (HDACs) are enzymes with a specialized function in tissue homeostasis and development[6]. HDACs have been separated into four classes based on their evolutionary similarity: Class I (HDACs 1, 2, 3, 8); Class II (HDACs 4, 5, 6, 7, 9, 10); Class III HDACs (SIRT1-7); and Class IV (HDACs 11)[7]. HDACs have significant therapeutic aims for cancer and neurological diseases[8]. Uncontrolled growth occurs in cancer as a result of deregulation of HDAC activity[9]. From the literature, the DFT based and *in vitro* mechanisms of cinnamomum exhibiting HDAC8 inhibitory activity have been reported[10].

However, no quantum chemical works have been carried out on *trans*-4-(trifluoromethyl) cinnamic acid (4TFCA). Therefore, in this study, the analysis on molecular structure of 4TFCA using DFT method has been performed. The most popular technique for performing structure calculations in quantum chemistry is DFT, which can yield information about electronic, vibrational and structural details of the molecule[11,12]. In DFT computations, Becke's three parameter exchange relations (B3) and the Lee Yang Parr (LYP) functional are very active, which enhances electron density calculations[13]. The theoretical vibrational assignments, molecular reactivity sites and the molecular geometric configuration of 4TFCA have been studied using the DFT/B3LYP method with 6-311++G(d,p) basis set, which is useful for enhancing the efficiency of polar bonds of carbon rings[14]. Initially, the molecular structure was optimized, and after that the vibrational assignments were done. The other molecular quantities such as molecular energy gap, molecular potential, Mullikan charge population, nuclear magnetic chemical shifts, molecular absorption, and natural bond orbital (NBO) calculations have been performed. Molecular docking

(MD)[15] is one of the computational method and it is a benefit tool for new drug detection and advanced medical research. Therefore, the molecular docking studies of 4TFCA have been achieved with histone deacetylases (HDAC8) inhibitor. ADMET (Absorption, Distribution, Metabolism, Excretion, Toxicity)[16] is a fast mode to find if a molecule has appropriate pharmacokinetics properties. Hence, using the *in silico* ADMET estimate tool, the toxicity of the system has been measured.

Experimental Method

Experimental Characterizations

The 4TFCA was obtained from Sigma Aldrich Chemicals in the United States for the purpose of recording the spectrum. The sample's FTIR was captured using a Perkin Elmer FTIR spectrometer and a KBr pellet with a resolution of 1.0 cm^{-1}. The sample's FT- Raman band was observed using a BRUKER RFS 27 spectrometer model with a resolution of 2 cm^{-1}. The FTIR and FT-Raman scales were investigated in the 4000-400 cm^{-1} and 4000-50 cm^{-1} wavenumber ranges, respectively. The spectroscopic vibrational characterizations are used to check the functional groups of the molecule.

Quantum Chemical Calculations

The computational studies such as molecular optimization, minimum energy, thermodynamical properties, vibrational wavenumbers calculations, IR intensity, Raman activity and the force field calculations are done by using GAUSSIAN 09W program[17]. DFT calculations of 4TFCA molecule have been achieved by the B3LYP functional with 6-311++G(d,p) basis set and electronic properties have been visualized by Gaussview 05 program[18]. By using a scale factor[19] of 0.9613 for the B3LYP method, the scaled frequencies were obtained which ensures the better agreement between experimental and DFT calculated values. Sundius's MOLVIB software[20] (Adaptation V7.0-G77) is used to calculate the potential energy distribution (PED) for various vibrational modes.

Molecular Docking and ADMET Prediction

The Protein Data Bank (http://www.pdb.org) was used to obtain the protein structures[21]. The molecule was selected as a ligand, and its structure was found from open ligand datafiles: PubChem (http://pubchem.ncbi.nlm.nih.gov/)[22]. The Discovery Studios (Adaptation: 2017 R2 client)[23] programme was used to evaluate the protein structure and amino acid corrosive location *via* docking relation with the molecule. Auto Dock Vina is utilized to perform the docking calculations (Adaptation: 4.2.1)[24].

ADMET properties and drug-likeness of 4TFCA are predicted using computational techniques. The pharmacokinetic profile of the molecule was evaluated using the pkCSM-pharmacokinetics web server (http://biosig.unimelb.edu.au/pkcsm/prediction) and the ADMET-SAR prediction tool (http://lmmd.ecust.edu.cn/admetsar2/)[16].

Results and Discussion

Molecular Geometry Analysis

The optimized global energy for 4TFCA is found as –835.50925198 Hartrees. Fig. 1 displays the structure that has been optimized for 4TFCA. It has C_1 symmetry, contains an alkene double bond, a benzene ring and an acrylic acid group in the ring. The computed carbonyl bond lengths for C19-O20, C19-O21 found at 1.202 Å, 1.363 Å which are in well agreement with the corresponding experimental XRD[25,26] data of 1.234 Å, 1.368 Å. In general, the calculated bond distances differ from the experimental parameters because the experimental results were obtained in the solid state while the computed results were assessed in the gas state. The bond lengths of C2-H7, C3-H8, C5-H9, C6-H9, C6-H10, C15-H16, C17-H18 are calculated as 1.083 Å, 1.082 Å, 1.082 Å, 1.082 Å, 1.084 Å, 1.087 Å, 1.086 Å by B3LYP and their corresponding experimental values are found at 0.982 Å, 0.978 Å, 1.092 Å, 1.092 Å, 1.087 Å, 0.986 Å, 0.983 Å. The reductions in C-H bond lengths are due to the increase of their force constants. The C-C bond lengths in the aromatic ring have a slight deviation; because

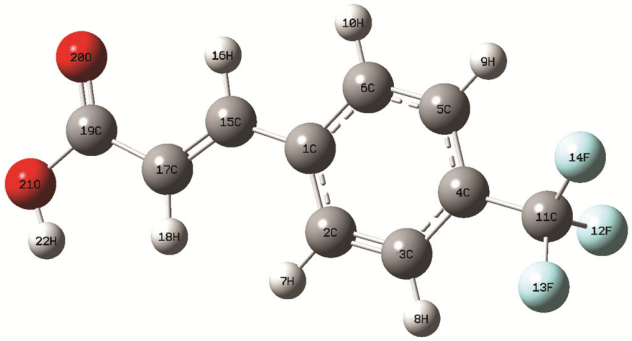

Fig. 1 — Optimized structure of *trans*-4-(trifluoromethyl)cinnamic acid

Table 1 — Optimized geometrical parameters of *trans*-4-(trifluoromethyl) cinnamic acid.

Parameters	Method/Basis set	Experimental*	Parameters	Method/Basis set	Experimental*
	DFT-B3LYP/ 6-311++G(d,p)			DFT-B3LYP/ 6-311++G(d,p)	
Bond length (Å)			C4-C3-H8	119.8	119.8
C1-C2	1.405	1.412	C3-C4-C5	120.0	121.6
C1-C6	1.403	1.401	C3-C4-C11	119.6	119.3
C1-C15	1.463	1.453	C5-C4-C11	120.2	121.7
C2-C3	1.385	1.372	C4-C5-C6	119.6	118.6
C2-H7	1.083	0.982	C4-C5-H9	120.1	121.8
C3-C4	1.398	1.384	C6-C5-H9	120.1	120.3
C3-H8	1.082	0.978	C1-C6-C5	121.2	122.4
C4-C5	1.393	1.387	C1-C6-H10	119.2	118.9
C4-C11	1.505	1.523	C5-C6-C10	119.4	118.9
C5-C6	1.390	1.378	C4-C11-F12	111.6	110.4
C5-H9	1.082	1.092	C4-C11-F13	112.0	111.8
C6-H10	1.084	1.087	C4-C11-F14	112.2	113.3
C11-F12	1.357	1.352	F12-C11-F13	106.5	105.3
C11-F13	1.352	1.358	F12-C11-F14	106.6	105.8
C11-F14	1.350	1.356	F13-C11-F14	107.2	105.4
C15-H16	1.087	0.986	C1-C15-H16	116.0	115.7
C15-C17	1.341	1.356	C1-C15-C17	127.8	128.7
C17-H18	1.086	0.983	H16-C15-C17	116.0	117.8
C17-C19	1.487	1.492	C15-C17-H18	121.6	122.1
C19-O20	1.202	1.234	C15-C17-C19	119.9	119.7
C19-O21	1.363	1.368	H18-C17-C19	118.3	118.6
O21-H22	0.964	0.982	C17-C19-O20	124.7	123.4
Bond angle (^{0})			C17-C19-O21	115.5	114.8
C2-C1-C6	118.1	119.3	O20-C19-O21	119.6	119.2
C2-C1-C15	123.3	121.7	C19-O21-H22	111.0	111.0
C6-C1-C15	118.4	117.2			
C1-C2-C3	120.9	121.7	Dihedral angle (^{0})		
C1-C2-H7	120.2	121.3	C6-C1-C2-C3	-0.0372	-0.0232
C3-C2-H7	118.8	117.2	C6-C1-C2-H7	179.87	176.87
C2-C3-C4	119.9	119.6	O20-C19-O21-H22	179.83	177.89
C2-C3-H8	120.1	121.9	C5-C4-C11-F14	28.8627	30.5679

*Experimental values from Ref. [25,26].

of the disorder in the fluorine groups and the electronegativity of oxygen atoms, its values are varied from 1.341 to 1.487 Å. These results show the small amount of electron-delocalization among the π-group of the benzene ring and the rest of the molecule. The C11-F12 bond length is calculated as 1.357 Å by B3LYP and the corresponding XRD data is found at 1.352 Å. The optimized and experimental geometrical parameters of 4TFCA are noted in Table 1. The calculated dihedral angle results clearly specify that the acid group and benzene ring are in the similar plane. The computed bond angles of C2-C1-C6, C4-C3-H8, O20-C19-O21 are calculated as 118.1°, 120.1°, 119.6° (corresponding experimental values: 119.3°, 121.9°, 119.2°). Table 2 provides a description of thermodynamic properties for 4TFCA. In this study, 2.8739 Debye is the extreme dipole moment of 4TFCA, which denotes a greater

Table 2 — The thermodynamic parameters of *trans*-4-(trifluoromethyl)cinnamic acid.

Parameters	DFT-B3LYP/ 6-311++G(d,p)
Optimized global minimum Energy (Hartrees)	–835.50925198
Total energy(thermal), E_{total} (kcal mol^{-1})	103.812
Heat capacity, C_v (cal mol^{-1} K^{-1})	48.827
Total Entropy, S (cal mol^{-1} K^{-1})	122.612
Translational Entropy (cal mol^{-1} K^{-1})	42.014
Rotational Entropy (cal mol^{-1} K^{-1})	32.680
Vibrational Entropy (cal mol^{-1} K^{-1})	47.918
Vibrational energy, E_{vib} (kcal mol^{-1})	102.034
Zero-point vibrational energy (kcal mol^{-1})	95.37866
Rotational constants (GHz)	
A	2.17377
B	0.19543
C	0.18520
Dipole moment (Debye)	2.8739

connection between the atoms of the molecule. The obtained total energy value for 4TFCA is found as 103.81 kcalmol^{-1} and the irrelevant vibrational energy (zero-point) of 95.39 kcalmol^{-1} is attained. These findings might influence the chemical reactions of 4TFCA.

Vibrational Assignments

4TFCA has 22 atoms, and leads its 60 normal modes, which are active in both the IR and Raman. Fig. 2 and 3 represent the computational and experimental spectra of 4TFCA. Table 3 illustrates the peak strengths and vibrational wavenumbers of 4TFCA. For heterocyclic compounds, the O-H stretching[27] vibrations are noted in the range 3670-3580 cm^{-1}. As a result, the O-H vibration is obtained as a weaker band for 4TFCA at 3612 cm^{-1} (99% PED) in the FTIR spectrum. The O-H bending frequencies of 4TFCA are also recognized and are in good consistent with the literature.

The stretching C-H vibrations[28] are formed among 3100-3000 cm^{-1}. The computational frequencies at 3079, 3078, 3061, 3055, 3032 and 3025 cm^{-1} with more than 90% PED are attributed to the C-H stretching vibrations of 4TFCA. The corresponding experimental vibrations are observed in IR at 3066, 3054, 3011, 2957, 2901, 2899 cm^{-1} and in FT-Raman at 3072, 3058, 3017, 2998, 2906, 2893 cm^{-1}. The C-H bending[29] frequencies of 4TFCA are also reported in Table 3. The stretching C-C frequencies play the crucial role in the substituted aromatic structure. Generally, C-C assignments[30] are exhibited in the range 1624-726 cm^{-1}. The experimental peaks in IR at 1619, 1527, 1502, 1477, 1312, 1301, 1299, 1291, 1221, 1122, 1111 cm^{-1} and Raman at 1627, 1529, 1508, 1486, 1321, 1307, 1293, 1286, 1214, 1131, 1102 cm^{-1} are assigned to C-C vibrations with 72-85% PED in 4TFCA. The equivalent DFT wavenumbers are found at 1614, 1589, 1544, 1485, 1387, 1306, 1303, 1287, 1224, 1161, 1118 cm^{-1}. The C=O[31] vibrations are commonly identified in the frequencies range 1780-1700 cm^{-1}. As a result, the experimental stretching C=O vibration of 4TFCA is noted in the FTIR at 1712 cm^{-1} and in the FT-Raman spectrum at 1721 cm^{-1}. The scaled C=O stretching is found as 1743 cm^{-1} for 4TFCA (86% PED). In general, the CF_3 stretching[32] vibrations are obtained in the range between 1100 and 1200 cm^{-1}. In this work, the fluorine in-plane stretching wavenumber (72% PED) is computed at 1260 cm^{-1} which matches with the experimental modes at 1253 and 1245 cm^{-1}. The CF_3 bending modes for 4TFCA are consistent with the previous report and are reported in Table 3.

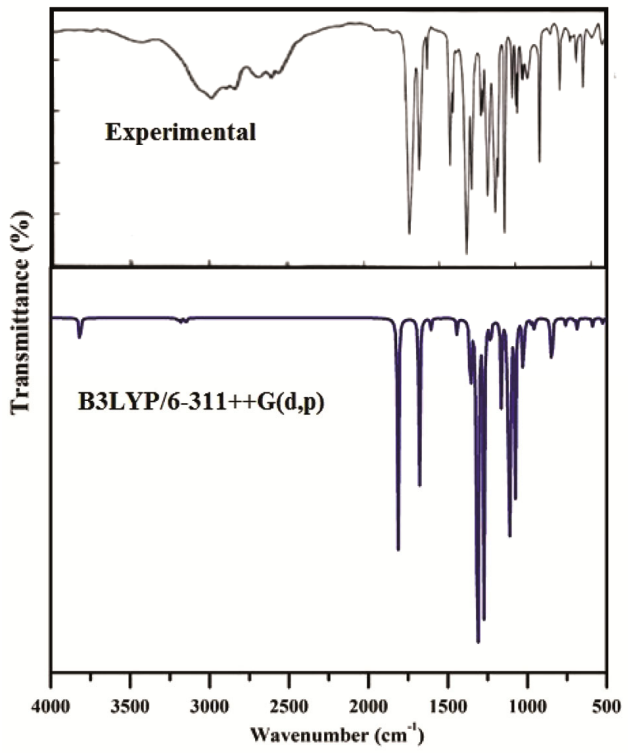

Fig. 2 — FTIR spectrum of *trans*-4-(trifluoromethyl)cinnamic acid

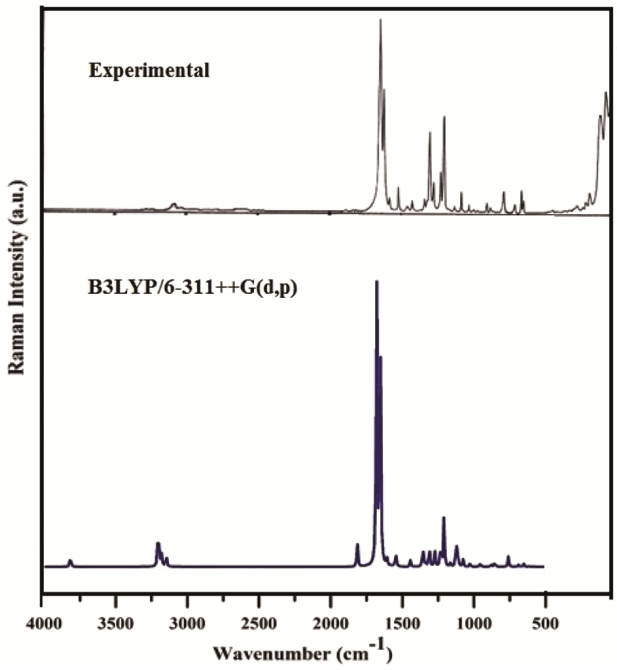

Fig. 3 — FT-Raman spectrum of *trans*-4-(trifluoromethyl) cinnamic acid

Table 3 — The vibrational frequencies (cm^{-1}), IR intensity (Km mol^{-1}) and Raman Activity ($Å^4$ amu^{-1}) for *trans*-4-(trifluoromethyl) cinnamic acid.

S. No	Observed wave number		Wave number (cm^{-1})		IR Intensity	Raman activity	Reduced mass	Force constant	Assignment with PED (%)
	FT-IR	FT- Raman	Calculated	Scaled					
1	3612(vw)	-	3816	3668	43.327	72.7073	1.0661	9.1469	νO-H (99)
2	3066(ms)	3072(vw)	3203	3079	0.2405	211.3028	1.0947	6.6201	νC-H (98)
3	3054(ms)	3058(vw)	3202	3078	3.0303	36.5495	1.0935	6.6089	νC-H (96)
4	3011(ms)	3017(vw)	3185	3061	4.1454	29.4368	1.0878	6.5019	νC-H (95)
5	2957(ms)	2998(vw)	3179	3055	3.0311	52.5533	1.0895	6.4879	νC-H (94)
6	2901(ms)	2906(vw)	3155	3032	2.4325	5.8165	1.0863	6.3717	νC-H (90)
7	2899(ms)	2893(vw)	3147	3025	5.2862	58.9441	1.0925	6.3778	νC-H (92)
8	1712(vs)	1721(vw)	1814	1743	307.4326	87.904	9.7008	18.8201	νC=O (88)
9	1619(ms)	1627(vs)	1679	1614	229.8677	1112.539	5.7356	9.5354	νC-C (85)
10	1527(ms)	1529(vs)	1653	1589	0.3063	958.1255	5.6608	9.1198	νC-C (86)
11	1502(w)	1508(vs)	1607	1544	14.4074	25.0912	6.3859	9.7211	νC-C (82)
12	1477(ms)	1486(ms)	1545	1485	0.6274	49.8613	2.4895	3.5052	νC-C (81)
13	1312(vs)	1321(ms)	1443	1387	18.8534	21.788	2.8242	3.4653	νC-O (80)
14	1301(vs)	1307(ms)	1359	1306	66.0758	17.6741	1.82	1.9814	νC-C (83)
15	1299(ms)	1293(ms)	1356	1303	55.4438	49.4591	1.7124	1.8555	νC-C (80)
16	1291(ms)	1286(ms)	1339	1287	3.5049	13.1982	1.7643	1.8658	νC-C (78)
17	1254(ms)	1259(ms)	1320	1268	187.8917	5.0369	3.6416	3.741	CF_{3ss} (75)
18	1253(ms)	1245(ms)	1311	1260	515.8462	66.7317	4.6629	4.7277	CF_{3ips} (72)
19	1221(ms)	1214(ms)	1274	1224	370.3826	49.6264	1.5165	1.4508	νC-C (78)
20	1198(vs)	1199(ms)	1232	1184	38.7658	86.6289	1.7807	1.5942	bO-H (76)
21	1122(vs)	1131(vw)	1208	1161	1.0161	155.9702	1.1997	1.0329	νC-C (74)
22	1111(vs)	1102(vw)	1164	1118	99.4871	9.5234	2.3101	1.8472	νC-C (72)
23	1087(vs)	1094(vw)	1124	1080	71.5974	65.1233	2.6204	1.9513	bC-H (70)
24	1071(vs)	1069(vw)	1117	1073	148.2375	42.4611	2.1466	1.5781	bC-H (71)
25	1061(vs)	1064(vw)	1108	1065	276.7734	14.5729	11.5764	8.3796	bC-H (72)
26	1024(vs)	1012(vw)	1075	1033	203.5658	21.2577	4.0724	2.7754	bC-H (69)
27	998(ms)	991(vw)	1029	989	49.9764	7.7116	3.669	2.2917	bC-H (70)
28	974(ms)	979(ms)	1018	978	30.2859	1.8741	1.2021	0.7352	bC-H (71)
29	950(ms)	948(ms)	990	951	0.5999	0.0307	1.3677	0.7909	Rasymd (68)
30	947(ms)	941(ms)	973	935	7.2736	0.3285	1.3172	0.7355	Rsymd (69)
31	921(ms)	924(ms)	955	918	16.5299	10.4008	4.3183	2.3218	Rtrigd (66)
32	867(ms)	869(ms)	880	845	0.4566	7.7787	1.8436	0.8413	bC-C (68)
33	833(ms)	838(ms)	856	822	11.1926	10.886	5.5631	2.4043	bC-C (65)
34	808(ms)	801(ms)	847	814	43.1803	2.5255	1.5476	0.6547	bC-C (62)
35	791(ms)	799(ms)	844	811	35.5043	0.4456	1.4544	0.6106	bC-C (64)
36	766(vs)	759(ms)	761	731	0.6804	8.3891	5.4402	1.8607	bC=O (65)
37	753(ms)	748(ms)	759	729	8.1651	22.6719	8.5854	2.9152	bC-O (63)
38	698(ms)	691(ms)	704	676	2.4177	0.4012	3.3413	0.978	ωC-H (61)
39	643(ms)	636(vw)	686	659	14.8038	6.1455	8.9185	2.4748	ωC-H (60)
40	621(ms)	624(vw)	650	624	0.4751	8.9268	7.1127	1.775	CF_{3ops} (62)
41	598(ms)	595(vw)	617	593	0.7238	1.6831	8.0024	1.7987	ωC-H (64)
42	552(ms)	557(vw)	589	566	9.9017	0.4919	4.086	0.8377	CF_{3ipb} (67)
43	532(mS)	538(vw)	572	549	0.4291	0.6726	10.3289	1.9964	CF_{3sb} (69)
44	497(ms)	503(vw)	526	505	6.0977	0.5525	4.7599	0.7775	ωC-H (67)
45	491(ms)	496(vw)	504	484	2.1681	0.5675	4.3398	0.6497	ωC-H (68)
46	438(ms)	431(vw)	425	408	35.006	1.2139	2.0113	0.2145	ωC-H (64)
47	391(ms)	396(vw)	410	394	8.2691	1.0614	4.1945	0.4165	CF_{3ipr} (69)
48	386 (ms)	394(vw)	406	390	5.1558	0.4284	3.323	0.3229	tRsymd (59)
49	377(ms)	368(vw)	391	375	55.5613	0.2766	2.5383	0.2295	tRasymd (58)
50	354(ms)	357(vw)	386	371	18.0611	0.3228	5.7775	0.5075	tRtrigd (60)
51	299(ms)	283(vw)	297	285	12.8856	1.0507	6.5755	0.3427	ωO-H (61)
52	231(vw)	241(vw)	256	246	3.7913	0.3267	5.166	0.2008	ωC-C (59)
53	-	188(ms)	205	197	0.3114	4.0889	10.9498	0.2724	ωC-C (58)
54	-	166(ms)	178	171	1.647	1.9283	9.0884	0.1703	ωC-C (56)

(*Contd*.)

Table 3 — The vibrational frequencies (cm^{-1}), IR intensity (Km mol^{-1}) and Raman Activity ($Å^4$ amu^{-1}) for *trans*-4-(trifluoromethyl) cinnamic acid. (*Contd.*)

S. No	Observed wave number		Wave number (cm^{-1})		IR Intensity	Raman activity	Reduced mass	Force constant	Assignment with PED (%)
	FT-IR	FT- Raman	Calculated	Scaled					
55	-	133(ms)	129	124	1.5516	2.3176	8.0592	0.0797	ωC-C (60)
56	-	84(ms)	77	74	4.6556	0.3265	6.5604	0.0234	CF_{3opr} (62)
57	-	78(ms)	75	72	0.6757	0.9731	2.9687	0.01	ωC=O (57)
58	-	47(ms)	45	43	9.5061	0.6033	8.8113	0.0107	ωC-O (58)
59	-	15(ms)	19	18	0.0849	2.0804	5.071	0.0011	CF_{3opb} (56)
60	-	12(ms)	14	13	1.6226	1.7374	6.465	0.0009	$CF_{3torsion}$ (55)

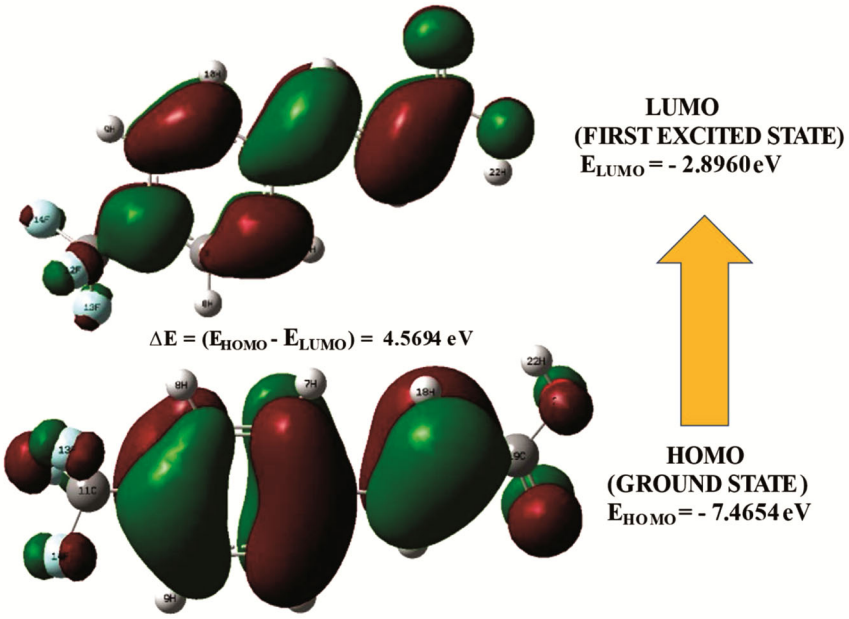

Fig. 4 — HOMO-LUMO plot of *trans*-4-(trifluoromethyl)cinnamic acid.

HOMO-LUMO Characterization

The excitation energies can be calculated in a variety of ways and the most basic is the difference among a neutral system's such as highest occupied molecular orbital (HOMO) and lowest unoccupied molecular orbital (LUMO). The HOMO-LUMO energy values, as well as their molecular orbital energy gap, reflect the molecule's chemical action. Also, the energy gap among both the HOMO-LUMO has explored intra-molecular charge exchange and bioactivity. Fig. 4 represents the calculated HOMO-LUMO energies for 4TFCA using the B3LYP/6-311++G(d,p) basis set. The computed HOMO energy value is –7.4654 eV that reveals the possibility of the electron donor (C-F and C-O bond of ring). The LUMO energy is computed as –2.8960 eV which suggest the leading most important electron acceptor (C-C bond of ring) and energy gap is calculated as 4.5694 eV. Further, the different molecular properties can be clarified by using Koopman's relations[33]. The chemical characteristics are provided in Table 4. The lowest energy gap and highest electrophilicity implies the strong chemical stability of 4TFCA.

Table 4 — Global reactivity descriptors for *trans*-4-(trifluoromethyl) cinnamic acid.

Molecular Properties	B3LYP/6-311++G(d,p)
HOMO (eV)	–7.4654
LUMO (eV)	–2.8960
Homo-Lumo gap (ΔE) (eV)	4.5694
Ionization potential (I) (eV)	7.4654
Electron affinity (A) (eV)	2.8960
Global hardness (η) (eV)	2.2847
Global softness (s) (eV^{-1})	0.2188
Electronegativity (χ) (eV)	5.1807
Chemical potential (μ) (eV)	–5.1807
Global electrophilicity (w) (eV)	11.7475

UV-Vis Analysis

UV-Visible spectral study has been investigated theoretically to evaluate the electronic properties of molecule and the TD-DFT[34] design is a valuable tool

for studying the static assets of molecule by using the excitation energies. Hence, the UV-Visible spectra of 4TFCA are simulated to identify the electronic shifts of molecule using time dependent TD-DFT/B3LYP method with higher basis set. A very solid peak is calculated by TD-DFT method at 477.50 nm with energy E = 2.5966 eV and oscillator frequency of 0.0215 for 4TFCA. This represents the transition that take place from HOMO to LUMO (93% contribution) and belongs to π →π* type. The electronic spectra of 4TFCA are illustrated in Fig. 5. The excitation energy has been computed at 323.49 nm with frequency f = 0.0017, E = 3.8327 eV from H-1→ L (π →π* type) with contribution of 91% as recorded in Table 5.

Mulliken Population (MC) Analysis

MC analysis[35] is one of the most commonly used population analysis for understanding the electron density of molecular systems. Fig. 6 plots the charge distribution in 4TFCA using B3LYP with the 6-311++G(d,p) basis set, and results are given in Table 6. The negative reactive responses for 4TFCA have been computed for the carbon atoms C2 (–0.9912), C3 (–0.5529), C4 (–0.5125), C5 (–0.2709), C6 (–0.0538), C17 (–0.0335), C19 (–0.0959) as well as the fluorine atoms F12 (–0.0656), F13 (–0.1066), F14 (–0.1095), the oxygen atoms O20 (–0.2795) and O21 (–0.1557). These are due to the carbon bonds connected with the greater electronegativity of oxygen and fluorine atoms. The four hydrogen atoms H22 (0.2535), H8 (0.1968), H9 (0.1897), and H16 (0.1819) have a higher positive charge compared to the other hydrogen atoms, since, these H atoms are placed close to oxygen and fluorine (O20, O21, F12, F13 and F14) atoms.

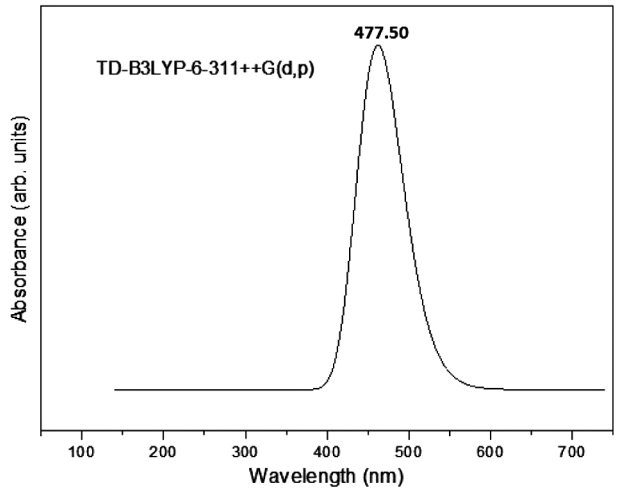

Fig. 5 — UV plot of *trans*-4-(trifluoromethyl)cinnamic acid

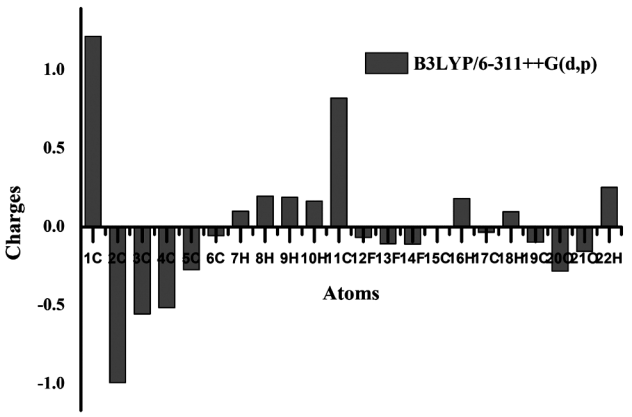

Fig. 6 — Mulliken charges plot for *trans*-4-(trifluoromethyl) cinnamic acid.

Table 6 — Mulliken's charge of *trans*-4-(trifluoromethyl) cinnamic acid.

Atom	Mulliken's atomic charges B3LYP/6-311++G(d,p)
1C	1.2165
2C	–0.9912
3C	–0.5529
4C	–0.5125
5C	–0.2709
6C	–0.0538
7H	0.1010
8H	0.1968
9H	0.1897
10H	0.1662
11C	0.8228
12F	–0.0656
13F	–0.1066
14F	–0.1095
15C	0.0007
16H	0.1819
17C	–0.0335
18H	0.0984
19C	–0.0959
20O	–0.2795
21O	–0.1557
22H	0.2535

Table 5 — Molecular orbital contributions of *trans*-4-(trifluoromethyl)cinnamic acid.

TDDFT/ B3LYP/6-311++G(d,p) Method

Energy(eV)	Oscillator strength	Wavelength (nm)	Major contributions	Assignment
2.5966	0.0215	477.50	H → L (93%)	π→π*
3.8327	0.0017	323.49	H-1 → L (91%)	π→π*

Molecular Electrostatic Potential (MEP)

The molecular electrostatic potential study has been utilized in pharmacology and biochemistry to identify the regions of negative and positive potential sites that either promote or inhibit certain types of biological activities[36]. The positive reactive sites are recognized for the nucleophilic action in the MEP plot, while the negative reactive sites are considered as the region of electrophilic attack. In Fig. 7, the MEP surface of 4TFCA is presented. The oxygen atom (O20) of 4TFCA (red region) is found as negative potential site. All hydrogens (blue region) in 4TFCA are identified as nucleophilic regions. This result established that the hydrogen and oxygen atoms in 4TFCA have the strongest attraction and repulsion sites, respectively.

Natural Bond Orbital (NBO) Analysis

The NBO approach is other beneficial tool to provide the information about connections in both filled and empty orbitals, which could help researchers to understand the intramolecular and intermolecular dynamics. Further, the conjugative interaction can be investigated more effectively using NBO analysis[37]. Table 7 provides the NBO results using the DFT/B3LYP/ 6-311++G(d,p) method for 4TFCA. In 4TFCA, the greater intra-molecular energy is found between the C1-C6 and C15-C17 orbitals with stabilization energy of 63.7 kcalmol^{-1}. In the ground state, the fluorine interaction with the ring system is highly difficult and leads to the stabilization of 5.35 kcalmol^{-1}. These interactions characterize the molecule to possess higher level of biological activity.

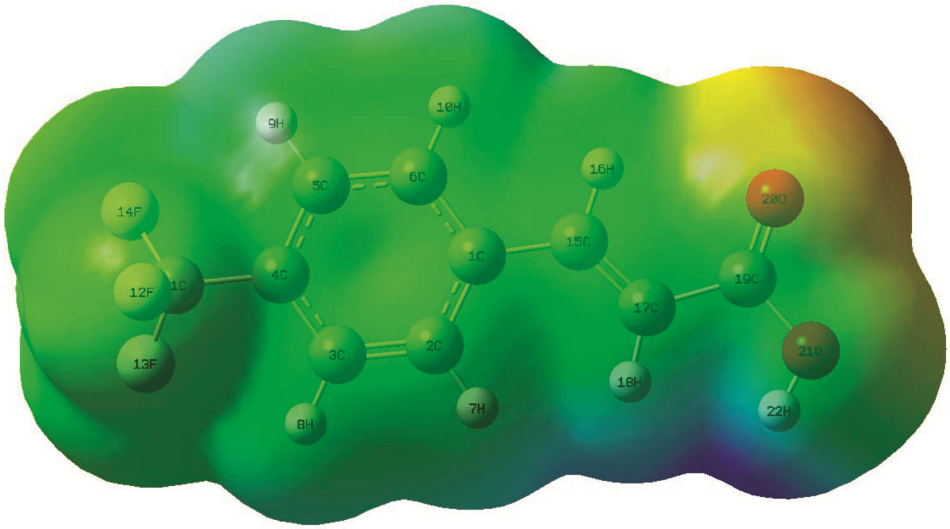

Fig. 7 — MEP plot for *trans*-4-(trifluoromethyl)cinnamic acid

Table 7 — Natural bond orbital analyses for *trans*-4-(trifluoromethyl)cinnamic acid.

Donor(i)	ED(i) (e)	Acceptor (j)	ED (j) (e)	Stabilization energy E(2) (kcal mol^{-1})	Energy difference E(j) - E(i) (a.u.)	Fock matrix element F (i,j) (a.u.)
π (C1-C6)	0.80529	π* (C2-C3)	0.14013	9.24	0.28	0.066
π (C1-C6)	0.80529	π* (C4-C5)	0.17734	10.82	0.28	0.07
π (C1-C6)	0.80529	π* (C15-C17)	0.04848	8.35	0.29	0.067
π (C2-C3)	0.83312	π* (C1-C6)	0.18042	9.96	0.29	0.068
π (C2-C3)	0.83312	π* (C4-C5)	0.17734	10.09	0.28	0.068
π (C15-C17)	0.93134	π* (C1-C6)	0.18042	5.66	0.31	0.056
π (C15-C17)	0.93134	π* (C19-O20)	0.12332	9.44	0.31	0.07
LP3 (F13)	0.96942	σ* (C11-F14)	0.04484	5.19	0.68	0.076
LP3 (F14)	0.96926	σ* (C11-F13)	0.04562	5.35	0.66	0.076
LP2 (O20)	0.91887	σ* (C17-C19)	0.03373	9.05	0.67	0.1
LP2 (O20)	0.91887	σ* (C19-O21)	0.05002	16.85	0.6	0.129
LP2 (O21)	0.91522	π* (C19-O20)	0.12332	20.46	0.35	0.109
LP2 (O21)	0.91522	σ* (O21-H22)	0.00388	8.94	2.15	0.183
π* (C1-C6)	0.18042	π* (C15-C17)	0.04848	63.7	0.01	0.067
σ* (C17-C19)	0.03373	σ* (C15-H16)	0.00858	6.75	0.02	0.067

NMR Analysis

NMR simulation is a capable way to identify the structural information of large biomolecules. In NMR spectral study, dimethyl sulfoxide (DMSO) is the generally used solvent because of its polarity. In addition, the oxygen atoms in DMSO cause strong hydrogen bonds with the acidic protons of solutes. The ^{13}C and ^{1}H NMR spectra for 4TFCA have been calculated using the DFT/ B3LYP/6-311++G(d,p) with gauge independent atomic orbital (GIAO) method[38]. Here, the chemical shift values have been computed by tetramethyl silane (TMS) as a reference. Table 8 presents the computed chemical shift results of 4TFCA. In Fig. 8, the calculated ^{13}C and ^{1}H NMR spectra are exposed. The calculated ^{13}C NMR shifts of 4TFCA are ranging from 170.54 (C19) to 120.44 (C17) ppm. In this study, the carbon atom (C19) attached with the high electronegative oxygen atom show the maximum NMR shift and the carbon atom (C17) associated to the H atoms of carbonyl group exhibit the lowest shift at 120.44 ppm. The lowest shifts are found in hydrogen atoms (H22 and H18) attached to oxygen atoms, which ranges from 6.53 to 6.62 ppm. The maximum shifts of 8.24, 8.23, 7.94, 7.80, 7.77 ppm are found at H16, H7, H9, H8, H10, respectively, which are directly connected to ring carbon atoms.

ADMET Prediction

Skin permeability, toxicity, human intestinal absorption (HIA) and blood-brain barrier (BBB) are used to determine the molecule's drug-likeness in the human body. The ADMET-SAR online software was used to assess the toxicity hazards and bioavailability of 4TFCA. Furthermore, the LD50 is an important parameter for predicting human lethal dose and killing after severe overdosing in humans[16]. In 4TFCA, the LD50 of 2.493 mol/kg have been determined. In this work, the human oral absorption of 4TFCA is identified as 91.56%. Furthermore, the approved range for the blood brain barrier (BBB) is –3.0 to 1.2; remarkably, the molecule 4TFCA shows the BBB permeability of 0.457 and the results indicating that the title molecule has good drug-like properties. Numerous ADMET limitations have also been obtained for 4TFCA and are exposed in Table 9.

Table 8 — ^{13}C and ^{1}H NMR chemical shifts for *trans*-4-(trifluoromethyl) cinnamic acid.

^{13}C Assignment	Calculated Shift B3LYP/6-311++G(d,p) (ppm)	^{1}H Assignment	Calculated Shift B3LYP/6-311++G(d,p) (ppm)
19C	170.54	16H	8.24
15C	156.52	7H	8.23
1C	142.93	9H	7.94
6C	139.33	8H	7.80
4C	138.38	10H	7.77
11C	134.20	18H	6.62
5C	131.89	22H	6.53
3C	131.30		
2C	130.74		
17C	120.44		

Molecular Docking (MD)

The most successful goals of pharmaceutical research have been achieved in the invention of new and improved drugs. MD is mainly used in pharmacological design, since the majority of drugs are made up of slight chemical components. It is an effective tool to find ligand-receptor relations. The AutoGrid 4.2 has been used to yield an affinity grid placed on the active site using a grid size of 120×120×120 with a strategy of 1.0 Å. The targeted rigid protein and flexible ligand docking has been completed with AutoDock 4.2.1. The ligand and

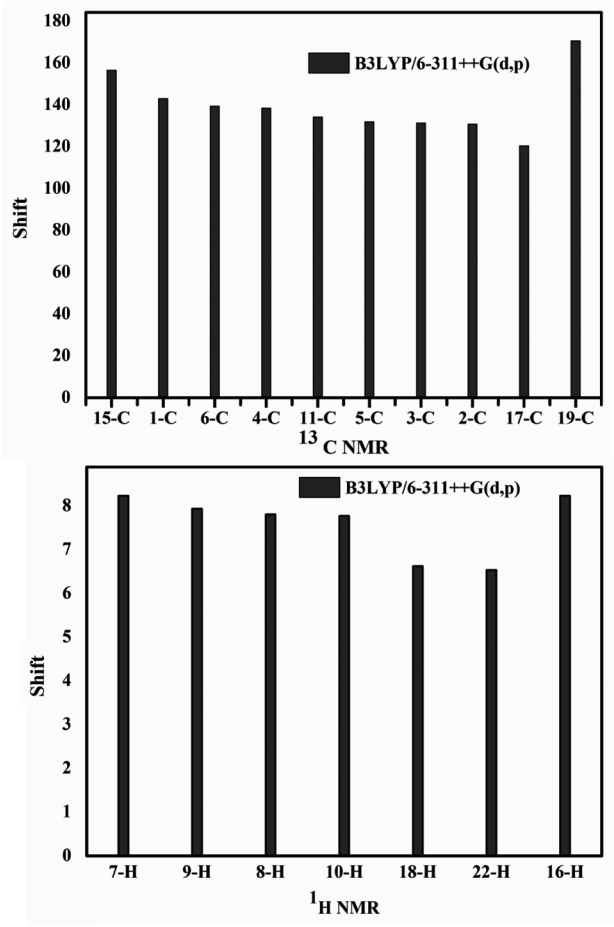

Fig. 8 — ^{13}C and ^{1}H NMR plot of *trans*-4-(trifluoromethyl) cinnamic acid.

Table 9 — ADMET profile of the *trans*-4-(trifluoromethyl)cinnamic acid.

ADMET prediction	Value	ADMET prediction	Value
CaCo-2 permeability (log Papp in 10^{-6} cm/s)	1.754	P-glycoprotein substrate	No
Intestinal absorption (human) (%)	91.56	P-glycoprotein I inhibitor	No
Skin Permeability (log Kp)	–2.7	P-glycoprotein II inhibitor	No
VDss (human) (log L/kg)	–1.1	Total Clearance (log ml/min/kg)	0.36
Fraction unbound (human) (Fu)	0.313	Renal OCT2 substrate	No
BBB permeability (log BB)	0.457	AMES toxicity test	No
CNS permeability (log PS)	–2.016	Max. tolerated dose (human) (log mg/kg/day)	0.936
CYP2D6 substrate	No	hERG I inhibitor	No
CYP3A4 substrate	No	hERG II inhibitor	No
CYP1A2 inhibitior	No	Oral Rat Acute Toxicity (LD50) (mol/kg)	2.493
CYP2C19 inhibitior	No	Oral Rat Chronic Toxicity (LOAEL) (log mg/kg_bw/day)	1.992
CYP2C9 inhibitior	No	Hepatotoxicity	No
CYP2D6 inhibitior	No	Skin Sensitisation	No
CYP3A4 inhibitior	No	T.Pyriformis toxicity (log ug/L)	No
Carcinogenicity	Non- carcinogens	Minnow toxicity (log mM)	1.52

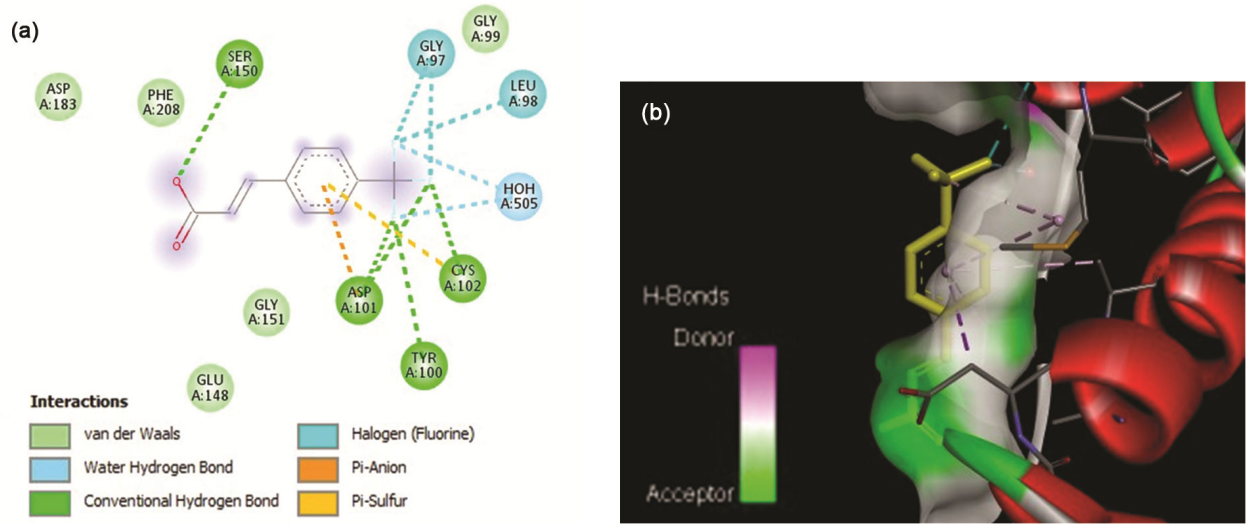

Fig. 9 — (a) 2D representation and (b) 3D interaction between the *trans*-4-(trifluoromethyl) cinnamic acid with HDAC8 (PDB ID: 1T67).

receptor structures were recorded in PDBQT setup for analyzing the docking energy affinities (kcal/mol). Finally, the docking values have been assessed by sorting the binding energy found from the docking confirmations. In addition, the 2D connections of protein and ligand molecule have been pictured by the Discovery Studio software.

Histone deacetylases (HDACs) are enzymes that eliminate acetyl groups from lysine's at histone N termini. This process increases chromatin condensation, which leads to transcriptional inhibition. HDACs over expression has been related to various forms of cancer, implying that HDAC inhibitors might be used in oncology[39].

In-silico studies revealed that 4TFCA interacts with histone deacetylases protein marker with protein ID: 1T67 as shown in Fig. 9(a) and 9(b). The binding energy of this protein is shown in Table 10(a). The present work exposed that 4TFCA binds with HDAC8 (hydrophobic interaction) at SER:150, ASP:101, CYS:102, TYR:100 as illustrated in Fig. 9(a) and Table 10(b). The docking binding energy (G°) of HDAC8 is found as –6.10 kcalmol^{-1}. Fig. 9(a) recognized that the oxygen and fluorine groups are associated with SER:150, PHE:208, LEU:98, GLY97 through π - π gathering and the hydrogen atoms in the benzene ring related with HOH 505. Hence, the HDAC8 has the extreme binding energies with 4TFCA on the dynamic binding responses. Therefore, it is sensible to hypothesize that 4TFCA may have prevailing histone deacetylases (HDACs) action.

Table 10(a) — Binding energy analysis (kcal/mol) of *trans*-4-(trifluoromethyl) cinnamic acid with HDAC8 inhibitor.

Protein	Binding Energy	Ligand Efficiency	Inhibit Constant	Internal energy	vdw hb dissolve energy	Electrostatic Energy	Total Internal	Torsinol Energy	Unbound Energy
HDAC8 (ID:1T67)	–6.10	–0.41	42.1	–5.31	–5.28	–0.21	–0.12	–1.01	–0.2

Table 10(b) — Docking calculation depicting interacting residues, binding site residues and atoms involved in H-bonding along with interacting residues.

S.No.	Protein	Interacted Residues	Ligand and Protein atom involved in H-bonding
1	HDAC8 (ID:1T67)	Asp 183, Phe 208, Ser 150, Gly 97, Gly 99, Leu 98, Hoh 505, Gly 151, Asp 101, Cys 102, Tyr 100, Glu 148	Ser 150, Asp 101, Cys 102, Tyr 100

Conclusions

Optimized structural parameters and computed normal modes of *trans*-4-(trifluoromethyl)cinnamic acid show well agreement with the experimental data. Molecular orbitals indicate that the molecule has more polarizable and good chemical responses. MEP defines the electrophilic (oxygen) and nucleophilic (hydrogen) responsive sites of the molecular system. The electronic absorbance of the molecule has also been matched well with the values of HOMO-LUMO. The structural information has been studied by NMR analysis. The NBO result indicates that the molecule has strong conjugative interaction. HDAC8 inhibitory demonstrated that the molecule 4TFCA is a potential bioactive agent with HDAC8 which results in greater binding energy (–6.10 $kcalmol^{-1}$). Highest LD50 results suggest that the molecule have minimum toxicity with more drug likeness. Therefore, both experimental and computed studies clearly reveal that the molecule 4TFCA has strong inhibitory activity against HDAC8 protein.

Acknowledgments

The authors would like to thank the management of Kalasalingam Academy of Research and Education, for providing the financial support to establish the computational research facility at the International Research Centre (IRC), Kalasalingam Academy of Research and Education.

References

1 Mathew S & Abraham, *Food Chem,* 94 (2006) 520.

2 Koppikar S J, Choudhari A S, Suryavanshi S A, Kumari S, Chattopadhyay S & Kaul-Ghanekar R, *BMC Cancer,* 10 (2010) 1.

3 Tung Y T, Chua M T, Wang S Y & Chang S T, *BioresourTechnol,* 99 (2008) 3908.

4 Matan N, Rimkeeree H, Mawson A J, Chompreeda P, Haruthaithanasan V & Parker M, *Int J Food Microbiol,* 107 (2006) 180.

5 Abu-Eittah R H, Khedr M K, Goma M & Zordok W, *Int J Quantum Chem,* 112 (2012) 1256.

6 Fischle W, Dequiedt F, Hendzel M J, Guenther M G, Lazar M A, Voelter W & Verdin E, *Mol Cell,* 9 (2002) 45.

7 Lahm A, Paolini C, Pallaoro M, Nardi M C, Jones P, Neddermann P, Sambucini S, Bottomley M J,Surdo P L, Carfí A, Koch U, Francesco R D, Hler C S & Gallinari P, *PNAS*, 104 (2007) 17335.

8 Vannini A, Volpari C, Filocamo G, Casavola E, Brunetti M, Renzoni D, Chakravarty P, Paolini C, Francesco R, Gallinari P, Steinkü C & Marco S D, *PNAS,* 101 (2004) 15064.

9 Senawong T, Misuna S, Khaopha S, Nuchadomrong S, Sawatsitang P, Phaosiri C, Surapaitoon A & Sripa B, *BMC Complement Med Ther,* 13 (2013) 1.

10 Patil M, Choudhari A, Pandita S, Islam M A, Raina P & Kaul-Ghanekar R, *Pharm Mag,*13 (2017) 645.

11 Becke A D, *J Chem Phys,* 98 (1993) 5648.

12 Kohn W, Becke A D & Parr R G, *J Phys Chem A,*100 (1996) 12974.

13 Premkumar S, Jawahar A, Mathavan T, Kumara Dhas M, Sathe V G & Milton Franklin Benial A, *Spectrochim Acta A Mol Biomol Spectrosc,* 129 (2014) 74.

14 Sundaraganesan N, Ilakiamani S, Subramani P & Joshua B D, *Spectrochim Acta A Mol Biomol Spectrosc*, 67 (2007) 628.

15 Chandrasekaran K & Thilak Kumar R, *J Chem Pharm Res,* 8 (2016) 849.

16 Guerrab W, Jemli M, Akachar J, Demirtaş G,Mague J T, Taoufik J, Ibrahimi A,Ansar M, Alaoui K&Ramli Y, *J Biomol Struct Dyn,* 40 (2021) 1.

17 Frisch M J, Trucks G W, Schlegal H B, Scuseria G E , Robb M A , Cheeseman J R, Scalmani G, Barone V , Petersson G A, Nakatsuji H, Li X, Caricato M, Marenich A, Bloino J, Janesko B G, Gomperts R, Mennucci B, Hratchian H P, Ortiz J V, Izmaylov A F, Sonnenberg J L, Williams-Young D, Ding F, Lipparini F , Egidi F , Goings J, Peng B, Petrone A, Henderson T, Ranasinghe D, Zakrzewski V G , Gao J, Rega N, Zheng G, Liang W, Hada M, Ehara M, Toyota K, Fukuda R, Hasegawa J, Ishida M, Nakajima T, Honda Y, Kitao O, Nakai H, Vreven T, Throssell K, Montgomery J A, Peralta J E, Ogliaro F, Bearpark M, Heyd J J, Brothers E, Kudin K N, Staroverov V N, Keith T, Kobayashi R, Normand J, Raghavachari K, Rendell A, Burant J C, Iyengar S S, Tomasi J, Cossi M, Millam J M, Klene M, Adamo C, Cammi R, Ochterski J W, Martin R L, Morokuma K, Farkas O, Foresman J B & D Fox J, *Gaussian09*, Revision A.02, (Gaussian Inc, Wallingford CT) 2009.

18 Dennington R, Keith T A & Millam J M, *Gauss View*, Version 5, (Shawnee Mission, KS: SemichemInc) 2009).

19 Young D C, *Computational Chemistry: A Practical Guide for Applying Techniques to Real World Problems,* (John Wiley & Sons Ltd, New York) 2001.
20 Sundius T, *Vib Spectro,* 29 (2002) 89.
21 O'Boyle N M, Banck M, James C A, Morley C, Vandermeersch T & Hutchison G R, *J Chem Info,* 3 (2011)1.
22 Mohan U P, Kunjiappan S, Pichiah B P T & Arunachalam S, *3 Biotech,* 11 (2021) 1.
23 Narayana B L, Pran Kishore D, Balakumar C, Rao K V, Kaur R, Rao A R, Murthy J N & Ravikumar M, *Chem Biol Drug Des,* 79 (2012) 674.
24 Trott O & Olson A J, *J Comp Chem,* 31 (2010) 455.
25 Howard J A K & Sparkes H A, *Cryst Eng Comm,* 10 (2008) 502.
26 Bryan R F & Freyberg D P, *J Chem Soc Perkin Trans,* 2 (1975) 1835.
27 Pandimeena G, Premkumar R, Mathavan T & Benial A M F, *J Mol Struct,* 1231 (2021) 129996.
28 Jeyavijayan S & Arivazhagan M, *Indian J Pure & Appl Phys,* 50 (2012) 623.
29 Jeyavijayan S, Gobinath E, Viswanathan K & Kumar S J, *Indian J Pure & Appl Phys,* 56 (2018) 108.
30 Sivaraj G, Jayamani N & Siva V, *J Mol Struct,* 1240 (2021) 130530.
31 Ramuthai M, Jeyavijayan S & Naidu D J, *Polycycl Aromat Compd,* 42 (10) (2022) 6988.
32 Kreienborg N M&Merten C, *Phys Chem Chem Phys,* 21 (2019) 3506.
33 Sundaraganesan N, Elango G, Meganathan C, Karthikeyan B & Kurt M, *Mol Simul,* 35 (2009) 705.
34 Regiec A & Wojciechowski P, *J Mol Struct,* 1196 (2019) 370.
35 Jeyavijayan S, Ramuthai M & Palani Murugan, *Indian J Chem,* 61 (2022) 1205.
36 Noureddine O, Issaoui N & Al-Dossary O, *J King Saud Univ Sci,* 33 (2021) 101248.
37 Nsangou M, Dhaouadi Z, Jaïdane N & Lakhdar Z B, *J Mol Struct THEOCHEM,* 819 (2007) 142.
38 VijayaChamundeeswari S P, James Jebaseelan Samuel E & Sundaraganesan N, *Mol Simul,* 38 (2012) 987.
39 Somoza J R, Skene R J, Katz B A, Mol C, Ho J D, Jennings A J, Luong C, Arvai A, Buggy J J, Chi E, Tang J, Sang B C, Verner E, Wynands R, Leahy E M, Dougan D R, Snell G, Navre M, Knuth M W, Swanson R, McRee D E & Tari L W, *Structure,* 12 (2004) 1325.